arXiv:cond-mat/9711252v1 [cond-mat.mes-hall] 24 Nov 1997

Multi-band energy spectra of spin-1/2 electrons with two-dimensional magnetic modulations

Ming-Che Chang[1] and Min-Fong Yang[2]
[1] *Department of Physics, National Tsing Hua University, Hsinchu, Taiwan*
[2] *Center of General Education, Chang Gung University, Kweishan, Taoyuan, Taiwan*
(March 24, 2022)

Abstract

The energy spectra of spin-1/2 electrons under two-dimensional magnetic field modulations are calculated beyond the one-band approximation. Our formulation is generally applicable to a modulation field with a rectangular lattice symmetry. The field distribution within a plaquette is otherwise arbitrary. The spectra being obtained are qualitatively different from their electric modulated counterparts. Peculiar features of the spectra are that, for an electron with a g factor precisely being equal to two, no matter how strong the modulation is, the zero-energy level seems to be unaffected by the modulation and is separated from higher energy levels with a nonzero energy gap. Moreover, there is a two-fold degenerancy for all states with positive energies with respect to spin flip. These features agree with earlier analytical studies of the periodically magnetic modulated systems.

PACS numbers: 71.25-s, 73.20Dx, 74.60.-w

Typeset using REVTEX

I. INTRODUCTION

Due to the progress of the submicron technology, one begins to observe quantum behaviors in the transport measurements of the field modulated two-dimensional electron gas (2DEG). Much effort has been devoted to the study of the spectral and the transport properties of a 2DEG in a periodic *magnetic* field with a nonzero uniform background B_0. These studies can be divided into two classes, depending on whether the field modulation is one dimensional[1–9] or two dimensional.[10–15]

For a one-dimensional magnetic modulated (1DMM) system, there are two characteristic length scales: the magnetic length, $\lambda = \sqrt{\hbar/eB_0}$, associated with the uniform background B_0 and the period a of modulation. By varying the ratio λ/a, the electron mobility and the magnetoresistance oscillate between extrema.[1] The oscillating behavior of the latter is similar to the Weiss oscillation in a one-dimensional electric modulated (1DEM) 2DEG.[16] These oscillations manifest the variation of the band widths: the (longitudinal) conductivity is proportional to the width of the Landau-level (LL) broadening, which is an oscillating function of both λ/a and LL indices due to the field modulation. Under special conditions (the so-called flat band conditions), the band width can be zero and electrons become immobile. Besides the transport property, other aspects of the 1DMM system have also been studied, such as collective excitations,[2] inelastic light scatterings,[3] surface states,[4] effect of electron-electron interactions,[5] and the effect due to an additional two-dimensional electric modulation.[6] The 1DMM systems may also be used as spin polarizers for magnetic dipoles.[7] Recently, the 1DMM systems have been realized experimentally by covering a regular array of superconductor[8] or micromagnet[9] on the top of a 2DEG, in which the observed magnetoresistance oscillation agrees very well with the theoretical prediction.

For the two-dimensional magnetic modulated (2DMM) systems, the Landau levels are not only broadened but also split to several subbands with an intricate fractal structure.[10,11] This is similar to the Hofstadter spectra for the two-dimensional electric modulated (2DEM) systems.[17] In fact, within the one-band approximation, both spectra are exactly the same to linear order in modulation fields.[11,12] For a square lattice in the one-band approximation, a Landau band is split to p subbands when there are p/q (p and q are relative prime integers) flux quanta per plaquette. Previous calculations of the 2DMM systems are either restricted to the one-band approximation,[11] or to the multiband calculation but with a specific magnetic field such that the flux quantum per plaquette is one (or one half).[12,13] Other aspects of the 2DMM systems have been studied, such as the collective excitations[10] and the degeneracy of the ground states.[14,15] There are some recent attempts to observe the peculiar transport properties due to the fractal band structure. However, as far as we know, this goal has not been achieved for the 2DMM systems.[18]

In the present work, the energy spectra of a spin-1/2 2DEG under two-dimensional magnetic field modulations are calculated *beyond the one-band approximation*, in which the Zeeman term is also included. In most of the above studies, the Zeeman effect is not included, however. For the electric modulated systems, neglect of the Zeeman term is justified, because the periodic electric field does not couple to electron spin and this term only contributes to a constant energy shift, $(g_e e\hbar/4m)B_0\sigma_z$, where g_e is the electron g factor and σ_z is $+1(-1)$ for spin-up (spin-down) electrons. However, this is not the case

for the magnetic modulated systems. After deriving the multi-band Harper equation, which is generally applicable to magnetic modulations with *arbitrary* strength and shape, as long as the field has a rectangular lattice symmetry, we show that the inclusion of the Zeeman term leads to qualitative changes in the energy spectra. Particularly, when $g_e = 2$, the most disparate result occurs for the lowest energy level — it is *not* broadened by the field modulation, and is separated from higher energy bands by a finite gap. Moreover, there exists a two-fold degenerancy for all states with positive energies with respect to spin flip. These results agree with earlier mathematical analysis of the 2DMM systems.[14,19]

The paper is organized as follows: the multi-band formalism is presented in Sec. II; the band structure is presented in Sec. III; and Sec. IV is devoted to summary and discussions.

II. MULTI-BAND FORMALISM

A. Magnetic translation symmetry

We consider a 2DEG under the influence of a magnetic modulation with a rectangular symmetry. The Hamiltonian is

$$H = \frac{1}{2}\left(-i\frac{\partial}{\partial \mathbf{r}} + \mathbf{A}_0(\mathbf{r}) + \mathbf{a}(\mathbf{r})\right)^2 + \frac{g_e}{4}B(\mathbf{r})\sigma_z, \tag{1}$$

where $\mathbf{A}_0(\mathbf{r})$ and $\mathbf{a}(\mathbf{r})$ are the vector potentials for the uniform background field B_0 and the modulation field $b(\mathbf{r}) = B(\mathbf{r}) - B_0$, respectively. In this paper, unless specified explicitly, we choose $\lambda = \sqrt{\hbar/eB_0}$ as the unit of length, $\hbar\omega_c$ as the unit of energy ($\omega_c = eB_0/m$ is the cyclotron frequency), and B_0 as the unit of magnetic field. In the absence of modulation, the Hamiltonian H_0 can be solved exactly with eigenvalues $E_n^{(0)} = n + 1/2 + g_e\sigma_z/4$.[20] H can be expanded as $H_0 + H_1 + H_2 + H_\sigma$, where H_1 and H_2 are the terms linear and quadratic in the vector potential $\mathbf{a}(\mathbf{r})$, respectively, and $H_\sigma = (g_e/4)b(\mathbf{r})\sigma_z$ is the *modulated* Zeeman term. The vector potential $\mathbf{a}(\mathbf{r})$ can be Fourier decomposed as $\mathbf{a}(\mathbf{r}) = \sum_{\mathbf{g}\neq 0}\mathbf{a}_\mathbf{g}e^{i\mathbf{g}\cdot\mathbf{r}}$, where $\mathbf{g}$ are the reciprocal lattice vectors of the rectangular lattice. By choosing the Coulomb gauge, the Fourier components $\mathbf{a}_\mathbf{g}$ are equivalent to $ib_\mathbf{g}\mathbf{g}\times\hat{\mathbf{z}}/g^2$, where $b_\mathbf{g}$ are the Fourier components of $b(\mathbf{r})$ and $g = |\mathbf{g}|$ (not to be confused with the electron g factor g_e). It is convenient to rewrite the exponential $e^{i\mathbf{g}\cdot\mathbf{r}}$ as $e^{i\mathbf{g}\cdot\boldsymbol{\xi}}e^{i\mathbf{g}\cdot\mathbf{R}}$, where the electron coordinate $\mathbf{r}$ is decomposed into a fast-moving cyclotron coordinate $\boldsymbol{\xi}$ and a slow-moving guiding-center coordinate $\mathbf{R} = \mathbf{r} - \boldsymbol{\xi}$. (See Appendix A.) Then it can be shown that

$$H_1 = -\sum_{\mathbf{g}\neq 0}\frac{b_\mathbf{g}}{g^2}\frac{\partial e^{i\mathbf{g}\cdot\boldsymbol{\xi}\lambda}}{\partial\lambda}|_{\lambda=1}e^{i\mathbf{g}\cdot\mathbf{R}}. \tag{2}$$

Similarly,

$$H_2 = -\frac{1}{2}\sum_{\mathbf{g}\neq 0}\sum_{\mathbf{g}'\neq 0}\mathbf{g}\cdot\mathbf{g}'\frac{b_\mathbf{g}}{g^2}\frac{b_{\mathbf{g}'}}{g'^2}e^{i(\mathbf{g}+\mathbf{g}')\cdot\boldsymbol{\xi}}e^{i(\mathbf{g}+\mathbf{g}')\cdot\mathbf{R}}, \tag{3}$$

and

$$H_\sigma = \frac{g_e \sigma_z}{4} \sum_{\mathbf{g}\neq 0} b_{\mathbf{g}} e^{i\mathbf{g}\cdot\boldsymbol{\xi}} e^{i\mathbf{g}\cdot\mathbf{R}}. \tag{4}$$

Due to the underlying magnetic translation symmetry[21] of the Hamiltonian, it is convenient to diagonalize the Hamiltonian on a basis which respects this symmetry. The unperturbative basis can be constructed as follows. By choosing a Landau gauge with $\mathbf{A}_0(\mathbf{r}) = (-y, 0)$, the magnetic translation operators are

$$T_1 = e^{a_1 \partial/\partial x}, \quad T_2 = e^{a_2(\partial/\partial y - ix)}, \tag{5}$$

where a_1 and a_2 are the lattice constants for the rectangular lattice. It is not difficult to show that, if there are p/q flux quanta per plaquette with an area $a_1 a_2$, then T_1, T_2^q, and H mutually commute. This is also true for the unmodulated Hamiltonian H_0, of course. Thus we can construct the explicit form of the magnetic Bloch states for H_0, which are the common eigenstates of H_0, T_1 and T_2^q:[13]

$$|n, \mathbf{k}\rangle = \sum_{l=-\infty}^{\infty} \bar{d}_l e^{-i(q/p)k_2 a_2 l} |n, k_1 - \frac{2\pi}{a_1} l\rangle, \tag{6}$$

where n is the LL index, $\mathbf{k} = (k_1, k_2)$ is the magnetic Bloch momentum, $\bar{d}_l$ are complex coefficients that are periodic in l with period p (i.e., $\bar{d}_{l+p} = \bar{d}_l$), and $|n, k_1\rangle$ are the common eigenstates of H_0 and T_1.

Since both H and H_0 are diagonal with respect to $\mathbf{k}$, it is clear that for the modulation part $H' = H - H_0$, we have $\langle n, \mathbf{k}|H'|n', \mathbf{k}'\rangle = \langle n, \mathbf{k}|H'|n', \mathbf{k}\rangle \delta_{\mathbf{k},\mathbf{k}'}$. Therefore, the α-th eigenstate of H can be written as

$$|\alpha, \mathbf{k}\rangle = \sum_{n=0}^{\infty} \sum_{l=-\infty}^{\infty} d_{n,l}^{(\alpha)} e^{-i(q/p)k_2 a_2 l} |n, k_1 - \frac{2\pi}{a_1} l\rangle, \tag{7}$$

where the unknown coefficients $d_{n,l}^{(\alpha)}$, as $\bar{d}_l$ above, are periodic in l with period p. Basically, the strategy below is to diagonalize the Hamiltonian matrix on the unperturbed basis and to solve for its eigenvalues.

In deriving the matrix elements of the Hamiltonians in Eqs. (2)–(4) on the unperturbed basis, the expression $\langle n, k_1 - 2\pi l/a_1 | e^{i\mathbf{g}\cdot\boldsymbol{\xi}} e^{i\mathbf{g}\cdot\mathbf{R}} | n', k_1 - 2\pi l'/a_1\rangle$ will be encountered frequently, thus we focus on its derivation first. Firstly we rewrite the exponential in a slightly different form, $e^{i\mathbf{g}\cdot\boldsymbol{\xi}} e^{i\tilde{\mathbf{g}}\cdot\tilde{\mathbf{R}}}$, to connect with the magnetic translation symmetry, where $\tilde{\mathbf{g}} = \mathbf{g} \times \hat{\mathbf{z}}$ and $\tilde{\mathbf{R}} = \mathbf{R} \times \hat{\mathbf{z}}$. Since the two dynamical variables, $\boldsymbol{\xi}$ and $\tilde{\mathbf{R}}$, decouple and operate on different parts of the Hilbert space (see Appendix A), the matrix elements of $e^{i\mathbf{g}\cdot\boldsymbol{\xi}} e^{i\tilde{\mathbf{g}}\cdot\tilde{\mathbf{R}}}$ can be evaluated with the help of Eq. (A1). The result is

$$\left\langle n, k_1 - \frac{2\pi}{a_1} l \left| e^{i\mathbf{g}\cdot\boldsymbol{\xi}} e^{i\tilde{\mathbf{g}}\cdot\tilde{\mathbf{R}}} \right| n', k_1 - \frac{2\pi}{a_1} l' \right\rangle = \delta_{l,l'-\bar{l}} P_{k_1 l}(\mathbf{g}) U_{nn'}(\mathbf{g}), \tag{8}$$

where $\mathbf{g} = (g_1, g_2) = (2\pi\bar{l}/a_1, 2\pi\bar{m}/a_2)$, $P_{k_1 l}(\mathbf{g}) = e^{-\pi i \bar{l}\bar{m} q/p} e^{2\pi i k_1 \bar{m}/a_2} e^{-2\pi i \bar{m} l q/p}$, and $U_{nn'}(\mathbf{g}) = \langle n | e^{i\mathbf{g}\cdot\boldsymbol{\xi}} | n'\rangle$. The magnetic flux condition, $a_1 a_2 = 2\pi p/q$, has been used.

B. Multi-band Harper equation

When the energy eigenstate $|\alpha, \mathbf{k}\rangle$ is expanded on the basis of $|n, k_1 - 2\pi l/a_1\rangle$ using Eq. (7), the eigenvalue equation, $H|\alpha, \mathbf{k}\rangle = E_\alpha(\mathbf{k})|\alpha, \mathbf{k}\rangle$, takes the following form,

$$E_n^{(0)} d_{n,s}^{(\alpha)} + \sum_{n',l'} e^{-i(q/p)k_2 a_2 (l'-l)} \langle n, k_1 - \frac{2\pi l}{a_1} | H' | n', k_1 - \frac{2\pi l'}{a_1} \rangle d_{n',s'}^{(\alpha)} = E_\alpha d_{n,s}^{(\alpha)}, \tag{9}$$

where $l = pr + s$ and $l' = pr' + s'$. (r, s, r', and s' are all integers such that $0 \le s, s' < p$.) Firstly we need to calculate the matrix elements of H'. With the help of Eqs. (2)–(4) and (8), we have

$$\begin{aligned}
\left\langle n, k_1 - \frac{2\pi l}{a_1} | H_1 | n', k_1 - \frac{2\pi l'}{a_1} \right\rangle &= -\delta_{l,l'-\bar{l}} \sum_{\mathbf{g}\neq 0} \frac{b_\mathbf{g}}{g^2} P_{k_1 s}(\mathbf{g}) \frac{\partial U_{nn'}(\mathbf{g}\lambda)}{\partial \lambda}|_{\lambda=1}, \\
\left\langle n, k_1 - \frac{2\pi l}{a_1} | H_2 | n', k_1 - \frac{2\pi l'}{a_1} \right\rangle &= -\frac{1}{2} \delta_{l,l'-\bar{l}-\bar{l}'} \sum_{\mathbf{g}\neq 0} \sum_{\mathbf{g}'\neq 0} \mathbf{g}\cdot\mathbf{g}' \frac{b_\mathbf{g}}{g^2} \frac{b_{\mathbf{g}'}}{g'^2} P_{k_1 s}(\mathbf{g}+\mathbf{g}') U_{nn'}(\mathbf{g}+\mathbf{g}'), \\
\left\langle n, k_1 - \frac{2\pi l}{a_1} | H_\sigma | n', k_1 - \frac{2\pi l'}{a_1} \right\rangle &= \frac{g_e \sigma_z}{4} \delta_{l,l'-\bar{l}} \sum_{\mathbf{g}\neq 0} b_\mathbf{g} P_{k_1 s}(\mathbf{g}) U_{nn'}(\mathbf{g}).
\end{aligned} \tag{10}$$

Combining Eqs. (9) and (10), we finally obtain

$$\begin{aligned}
&E_n^{(0)} d_{n,s}^{(\alpha)} + \sum_{n'} \sum_{\mathbf{g}\neq 0} b_\mathbf{g} \mathcal{P}_{\mathbf{k}s}(\mathbf{g}) \left[-\frac{1}{g^2} \frac{\partial U_{nn'}(\mathbf{g}\lambda)}{\partial \lambda}|_{\lambda=1} + \frac{g_e \sigma_z}{4} U_{nn'}(\mathbf{g}) \right] d_{n',s+\bar{s}}^{(\alpha)} \\
&\quad - \frac{1}{2} \sum_{n'} \sum_{\mathbf{g}\neq 0} \sum_{\mathbf{g}'\neq 0} \mathbf{g}\cdot\mathbf{g}' \frac{b_\mathbf{g}}{g^2} \frac{b_{\mathbf{g}'}}{g'^2} \mathcal{P}_{\mathbf{k}s}(\mathbf{g}+\mathbf{g}') U_{nn'}(\mathbf{g}+\mathbf{g}') d_{n',s+\bar{s}+\bar{s}'}^{(\alpha)} = E_\alpha d_{n,s}^{(\alpha)},
\end{aligned} \tag{11}$$

where $\mathcal{P}_{\mathbf{k}s}(\mathbf{g}) = e^{-2\pi i k_2 \bar{l}/a_1} P_{k_1 s}(\mathbf{g}) = e^{i\mathbf{k}\cdot(\mathbf{g}\times\hat{\mathbf{z}})} e^{-ig_1 g_2/2} e^{-ig_2(2\pi s/a_1)}$. It is a multi-band generalization of the Harper equation[17] (see Eq. (13)), thus Eq. (11) is called as the multi-band Harper equation.[22] It has to be solved in conjunction with the following identities concering inter-LL transitions (for $n \ge n'$),

$$\begin{aligned}
U_{nn'}(\mathbf{g}) &= \sqrt{\frac{n'!}{n!}} \left(\frac{g_-}{\sqrt{2}} \right)^{n-n'} e^{-g^2/4} L_{n'}^{n-n'}, \\
\frac{\partial U_{nn'}(\mathbf{g}\lambda)}{\partial \lambda}|_{\lambda=1} &= \sqrt{\frac{n'!}{n!}} \left(\frac{g_-}{\sqrt{2}} \right)^{n-n'} e^{-g^2/4} \left[(n - n' - g^2/2) L_{n'}^{n-n'} - g^2 L_{n'-1}^{n-n'+1} \right],
\end{aligned} \tag{12}$$

where $g_- = g_1 - ig_2$ and $L_{n'}^{n-n'}$ ($L_{-1}^n = 0$) are the associated Laguerre polymials with the argument $g^2/2$.

Until now, no approximation has been used. This multi-band Harper equation applies to general shape of magnetic field distribution with a rectangular lattice symmetry. To simplify the calculation, from now on, we assume the spatial field modulation is $b(\mathbf{r}) = 2b_{10}[\cos(2\pi x/a) + \cos(2\pi y/a)]$ with a square lattice symmetry (i.e., $a_1 = a_2 = a$). In the numerical calculations, the eigenvalues are obtained by diagonalizing a $(1 + n_{\rm cut})p \times (1 + n_{\rm cut})p$ matrix, where the cut-off $n_{\rm cut}$ has to be large enough to ensure the eigenvalues being

obtained converge to the correct result. The precise spectra that include the effect of inter-LL transitions are shown in the next section.

Before closing this subsection, we show that, under the so-called one-band approximation, Eq. (11) can indeed be reduced to the usual Harper equation. When the inter-LL transitions and the terms quadratic in $b_{\mathbf{g}}$ are neglected, $d_{n,l}^{(\alpha)} \to \bar{d}_l \delta_n^\alpha$ (due to the periodicity, $\bar{d}_{l+p} = \bar{d}_l$, there are only p independent coefficients, i.e., $\bar{d}_0, \cdots, \bar{d}_{p-1}$), and then Eq. (11) is reduced to the one-band equation:

$$M_n\left(\frac{q}{p}\right)\left\{\bar{d}_{s-1}e^{2\pi i k_2/a} + \bar{d}_{s+1}e^{-2\pi i k_2/a} + 2\bar{d}_s \cos\left[2\pi\left(\frac{k_1}{a} - s\frac{q}{p}\right)\right]\right\} = \left[E_n\left(\frac{q}{p}\right) - E_n^{(0)}\right]\bar{d}_s, \tag{13}$$

where $M_n(q/p) = (b_{10}/2)[L_n^1 + L_{n-1}^1 + (g_e\sigma_z/2)L_n]e^{-g_{10}^2/4}$ is an overall factor that scales the energy, and $g_{10}^2 = (2\pi/a)^2 = 2\pi q/p$. Apart from the factor $M_n(q/p)$ where the spin-related term is included, Eq. (13) is precisely the same as the Harper equation for a 2DEM system.[17] The spectrum for $E_n(q/p)/M_n(q/p)$ within the one-band approximation is thus trivial:[11,12] irrespective of the LL index n, it is the usual Hofstadter spectrum calculated for a 2DEM system. There is one exception, however. When $n = 0$, $g_e = 2$, and $\sigma_z = -1$, $M_0(q/p)$ is equal to zero, and then $E_0(q/p) = E_0^{(0)}$, as if the field modulation exerts no influence at all. Actually, the equality $E_0(q/p) = E_0^{(0)}$ is valid even beyond the one-band approximation. This is discussed in more details in Sec. III.

III. FRACTAL BAND STRUCTURE

In this section we show the band structures for both weak and strong modulations. The influence of the Zeeman term is particularly emphasized. For an unmodulated 2DEG with no Zeeman effect, the energy spectrum consists of discrete, dispersionless LLs.[20] These LLs are highly degenerate because of the continuous translation symmetry, which gives an infinite degenerancy, and the spin-flip symmetry, which gives a two-fold degenerancy. When a periodic modulation is introduced, which breaks the continuous translation symmetry, we expect that the degenerancy for each LL will be lifted. Indeed, in the one-band approximation, one finds that each LL is broadened and split to several intricate energy subbands. The way these subbands split is the same for every LL in the one-band approximation (see the discussion at the end of the last section). However, when the inter-LL transitions are included, the exact calculations shown below reveal that the subband structures are actually different for different LLs, thus lead to much more complicated structures.

In Fig. 1, the spectrum of electrons with $g_e = 0$ under a weak square modulation field with $b_{10}a^2 = 0.2\phi_0$ (in the usual units, where $\phi_0 = h/e$ is the flux quantum) is shown. Because there is no Zeeman splitting, there is no need to distinguish the spin-up electrons from the spin-down electrons and the spectrum for only one spin direction is shown. The calculation is done with a cut-off $n_{\rm cut} = 9$. The result with a larger cut-off at $n_{\rm cut} = 14$ shows no visible difference from Fig. 1. Notice that the abscissa is the inverse of the magnetic flux, q/p. In this and the following figures, it is assumed that, while changing the magnetic flux by varying B_0, the modulation amplitude b_{10} is fixed. For the weak modulation case, the envelope for each

energy band is largely determined by the scaling factor $M_n(q/p)$. Obviously, some features specific to the one-band approximation no longer exist. For example, the interband couplings remove the symmetry of the butterfly diagram. Similar effect of symmetry breaking is also observed in the multi-band calculation for the 2DEM systems.[22]

The two-fold degenerancy for electron spin is lifted when the Zeeman effect is not negligible. In our 2DMM systems, the Zeeman effect does not only give an energy shift, but also induce inter-LL transitions (see Eq. (10) for H_σ). Thus, the interplay between the orbital effect (H_1+H_2) and the Zeeman effect (H_σ) leads to different spectral structures between the spin-up and the spin-down electrons, which are shown in Fig. 2. The spectrum in Fig. 2(a) (Fig. 2(b)) is for a spin-down (spin-up) electron with a g factor equals to one. It can be seen that, in addition to the overall constant Zeeman energy shift $g_e\sigma_z/4$ due to the background field, the spectra show qualitative differences from Fig. 1. For example, the structures for the second lowest energy bands near $q/p = 0.9$ in Figs. 2(a) and (b) are visibly different from that in Fig. 1, and are different from each other.

The spectrum in Fig. 3(a) (Fig. 3(b)) is for a spin-down (spin-up) electron with a g factor equals to two. For this particular g factor, two significant features are observed. The first is that the lowest energy level for a spin-down electron is flat and equals to zero to very high precision. The second is that the positive-energy spectrum is degenerate with respect to spin flip, whereas the flat band in Fig. 3(a) has no counterpart in Fig. 3(b). Both features persist for stronger modulations.

The two-fold degenerancy for the positive-energy states in the case of $g_e = 2$ indicates that there must be an additional symmetry even in the presence of the Zeeman term. It was pointed out by Aharonov and Casher[23] that this degenerancy results from a symmetry transformation which *simultaneously* changes the direction of the electron spin and the spatial dependence of the wavefunction. This symmetry can be related to the supersymmetry,[24] or to the chiral (γ_5) invariance by connecting our problem to the $(1+1)$-dimensional theory of Dirac fermions.[23]

Moreover, based on an abstract mathematical analysis, Dubrovin and Novikov showed that, for a spin-down electron with $g_e = 2$, there always exist the zero-energy states in the 2DMM systems, no matter how strong the modulation is.[14] Furthermore, by using topological arguements, they proved that, although the continuous translation symmetry is broken in the 2DMM system, the degenerancy of this zero-energy states is the *same* as that for the unmodulated system. One may wonder whether this unexpected degeneracy is symmetry-related and, if it is, what is the nature of this symmetry. In fact, it was shown by Gendenshtein that, because the Hamiltonian in Eq. (1) with $g_e = 2$ can be factorized into a product of two conjugate first-order differential operators,[23] such a symmetry is indeed present for the zero-energy states.[24] However, this is *not* a symmetry of the original Hamiltonian, but rather of one of the two first-order differential operators. (For more details, see Ref. [24].)

In comparison with the $g_e \neq 2$ cases, there is one more unique feature for the $g_e = 2$ case, which becomes obvious when the modulation is quite strong. Figs. 4(a) and (b) show the strongly modulated band structures of *spin-down* electrons with $g_e = 1$ and 2, respectively. The modulation strength is $b_{10}a^2 = 0.8\phi_0$. For the case of $g_e = 2$, besides the fact that the lowest energy level remains flat despite the strong mixing between the unperturbated LLs, it is apparent that the zero-energy level is isolated from the intermingled fractal structure

with a finite energy gap. This is true for even stronger modulations. On the contrary, such a behavior does not appear in Fig. 4(a) for the case of $g_e = 1$. A simple explanation of the gap above the flat band is as follows:[14] if the gap collapses at a particular modulation, such that a state from a higher energy band merges with the zero-energy one, then the degenerancy of the zero-energy states will increase by one. However, this is impossible because this degenerancy in the modulated system must be the same as that in the unmodulated one, as mentioned above.[14] Therefore, the flat band has to be separated from higher bands.

Fig. 5 shows the dependence of the energy bands on the g factor when the total flux per plaquette is $B_0a^2 = 1\phi_0$ and $b_{10}a^2 = 0.2\phi_0$. In this figure, the sign of the g factor refers to the direction of spins (+ for up, − for down). (Note that the sign convention for g_e applies only to Fig. 5, but not to the previous discussions.) It is clear that the lowest band is broadened as soon as $g_e \neq -2$. Notice that the spectrum for $g_e = 2$ and that for $g_e = -2$ are identical, except for the lacking of the flat band at zero energy for $g_e = 2$. In addition to the zero-energy flat band, the band widths of other energy bands can also shrink to zero at some particular values of g_e. For example, The width of the second lowest energy band is zero when $g_e = -0.12$. However, unlike the shrinking of the lowest band at $g_e = -2$, this 'pinch' point moves if a different flux value of B_0a^2 is chosen.

IV. SUMMARY AND DISCUSSIONS

In this paper, we present an accurate multi-band calculation of the energy spectra of the 2DMM spin-1/2 electronic systems, in which the Zeeman effect is also taken into account. We find that, when the Zeeman energy is not negligible, the spectra are changed qualitatively with respect to their electric modulated counterparts. Moreover, in the special case when the electron g factor is two, it is found that: 1. the positive-energy eigenstates have a two-fold degeneracy with respect to spin flip; 2. for the spin-down electrons, the ground states seem to be unaffected by the periodic modulation and remains highly degenerate even in very strong modulations; 3. the ground states are separated from higher energy states with a finite energy gap. However, these special properties no longer exist if the g factor is not equal to two.

In real systems, the electron g factor can be changed by either varying the width of a quantum well that holds the electrons,[25] or by applying a hydrostatic pressure[26] to the sample. Thus, it is possible to combine these two methods and to design an experiment in which the g factor can be continuously tuned around two.[26] Under such a circumstance, the peculiar and robust spectral properties of the lowest energy level should exhibit itself through the transport properties. Since the band splitting may suppress the band conductivity,[18] it is advised to keep the flux per plaquette at one or a simple fraction in order to observe the conductivity enhancement induced by level broadening away from $g_e = 2$, or, conversely, the conductivity reduction at $g_e = 2$.

However, most of current experiments can achieve only weak modulations. For example, consider a source of a periodic magnetic field, $B(\mathbf{r}) = B_0+(B_0/2)(\cos 2\pi x/a+\cos 2\pi y/a) \geq 0$. The field modulation felt by a 2DEG at a distance d below the source becomes $B_d(\mathbf{r}) = B_0 + (B_0e^{-2\pi d/a}/2)(\cos 2\pi x/a + \cos 2\pi y/a)$.[27] This corresponds to $b_{10} = e^{-2\pi d/a}/4$ in our calculation. For typical values such as $a = 1$ μm and $d = 10$ nm, b_{10} is equal to 0.23. The

optimum value of b_{10} is $1/4$, when $d = 0$. It can be larger than $1/4$ only if the amplitude of the modulation field is larger than the background field. In this case, the total field $B(\mathbf{r})$ reverses direction in some regions.

In the future, to bring theoretical results much closer to the real experiments, ingredients such as disorder and electron-electron interaction have to be included in the calculation. It may also be necessary to include an extra two-dimensional electric modulation, which is inevitably induced due to the strain exerted by the ferromagnetic or the superconductor grid at low temperatures in recent experiments.[8,9,11] It will be very interesting to investigate the influence of these factors on the energy spectra reported here.

ACKNOWLEDGMENTS

This work is supported by the National Science Council of Taiwan under contract No. 87-2112-M-007-008.

APPENDIX A: GUIDING-CENTER COORDINATE

In the semiclassical calculations of the transport properties of the quantum Hall systems, in which the applied magnetic field is strong and the disorder potential is smooth,[28] one usually decomposes the electron coordinate $\mathbf{r}$ into a fast-moving cyclotron coordinate, $\boldsymbol{\xi} = \hat{\mathbf{z}} \times (\mathbf{p} + \mathbf{A}_0)$, and a slow-moving guiding center, $\mathbf{R} = \mathbf{r} - \boldsymbol{\xi}$. In the present study, although the periodic field variation is not required to vary smoothly, the derivation of the multi-band Harper equation can be simplified with the help of this decomposition.

It can be shown that (ξ_1, ξ_2) and (R_1, R_2) are independent conjugate pairs respectively, i.e., $[\xi_1, \xi_2] = -i$, $[R_1, R_2] = i$, and $[\xi_i, R_j] = 0$ for $i, j = 1, 2$. Thus the exponential $e^{i\mathbf{g}\cdot\mathbf{r}}$ can be decomposed as $e^{i\mathbf{g}\cdot\boldsymbol{\xi}} e^{i\mathbf{g}\cdot\mathbf{R}} = e^{i\mathbf{g}\cdot\boldsymbol{\xi}} e^{i\tilde{\mathbf{g}}\cdot\tilde{\mathbf{R}}}$, where $\tilde{\mathbf{g}} = \mathbf{g}\times\hat{\mathbf{z}}$ and $\tilde{\mathbf{R}} = \mathbf{R}\times\hat{\mathbf{z}}$. For a Landau gauge with $\mathbf{A}_0(\mathbf{r}) = (-y, 0)$, we have $\boldsymbol{\xi} = (-i\partial_y, i\partial_x + y)$ and $\tilde{\mathbf{R}} = (-i\partial_x, -i\partial_y - x)$. Therefore, the magnetic translation operators in Eq. (5) can be rewritten as $T_j = e^{i\tilde{R}_j a_j}$, $j = 1, 2$. Consequently, we have the following very useful identities,

$$\begin{aligned} T_1|n, k_1\rangle &= e^{i\tilde{R}_1 a_1}|n, k_1\rangle = e^{ik_1 a_1}|n, k_1\rangle, \\ T_2|n, k_1\rangle &= e^{i\tilde{R}_2 a_2}|n, k_1\rangle = |n, k_1 - a_2\rangle. \end{aligned} \tag{A1}$$

The second equation is a direct result of the commutation relation between $\tilde{R}_1$ and $\tilde{R}_2$, $[\tilde{R}_1, \tilde{R}_2] = i$. Therefore, the 'rotated' guiding-center coordinate is the generator of the magnetic translation. It can be verified that $e^{i\tilde{R}_1 a_1}|n, \mathbf{k}\rangle = e^{ik_1 a_1}|n, \mathbf{k}\rangle$ and $e^{i\tilde{R}_2 q a_2}|n, \mathbf{k}\rangle = e^{iqk_2 a_2}|n, \mathbf{k}\rangle$ using Eq. (A1) and the periodicity of $\bar{d}_l$ (see Eq. (6)). Thus, $|n, \mathbf{k}\rangle$ are indeed the common eigenstates of H_0, T_1, and T_2^q. Similarly, due to the periodicity of $d_{n,l}^{(\alpha)}$ (see Eq. (7)), one can prove that the energy eigenstates $|\alpha, \mathbf{k}\rangle$ are also the eigenstates of T_1 and T_2^q.

REFERENCES

[1] D. P. Xue and G. Xiao, Phys. Rev. B **45**, 5986 (1992); F M. Peeters and P. Vasilopoulos, *ibid.* **47**, 1466 (1993); R. Yagi and Y. Iye, J. Phys. Soc. Japan **62**, 1279 (1993); I. S. Ibrahim and F. M. Peeters, Phys. Rev. B **52**, 17321 (1995); A. Krakovsky, *ibid.* **53**, 8469 (1996); Q. W. Shi and K. Y. Szeto, *ibid.* **55**, 4558 (1997).

[2] X. Wu and S. E. Ulloa, Phys. Rev. B **47**, 7182 (1993).

[3] H. L. Cui, Y. Fessatidis, and P. Vasilopoulos, Phys. Rev. B **52**, 13765 (1995).

[4] A. Akjouj and B. Djafari-Rouhani, Solid State Comm. **103**, 161 (1997).

[5] A. Manolescu and R. R. Gerhardts, cond-mat/9707292; U. J. Gossmann, A. Manolescu, and R. R. Gerhardts, cond-mat/9710052.

[6] G. Gumbs, D. Miessein, and D. Huang, Phys. Rev. B **52**, 14755 (1995); G. Y. Oh and M. H. Lee, *ibid.* **53**, 1225 (1996).

[7] A. O. Barut and J. P. Dowling, Phys. Rev. Lett. **68**, 3571 (1992).

[8] H. A. Carmona *et al.*, Phys. Rev. Lett. **74**, 3009 (1995).

[9] P. D. Ye *et al.*, Phys. Rev. Lett. **74**, 3013 (1995).

[10] X. Wu and S. E. Ulloa, Phys.Rev. B **47**, 10028 (1993).

[11] R. R. Gerhardts, Phys. Rev. B **53**, 11064 (1996); R. R. Gerhardts, D. Pfannkuche, and V. Gudmundsson, Phys. Rev. B **53**, 9591 (1996).

[12] D. Yoshiyoka and Y. Iye, J. Phys. Soc. Jpn. **87**, 448 (1987).

[13] M. C. Chang and Q. Niu, Phys. Rev. B **50**, 10843 (1994).

[14] B. A. Dubrovin and S. P. Novikov, Sov. Phys. JETP **52**, 511 (1980); Sov. Math. Dokl. **22**, 240 (1980); S. P. Novikov, Sov. Math. Dokl. **23**, 298 (1981).

[15] A. Y. Rom, Phys. Rev. B **55**, 11025 (1997).

[16] R. R. Gerhardts, D. Weiss, and K. von Klitzing, Phys. Rev. Lett. **62**, 1173 (1989); R. W. Winkler, J. P. Kotthaus, and K. Ploog, *ibid.* **62**, 1177 (1989); P. Vasilopoulos and F. M. Peeters, *ibid.* **63**, 2120 (1989); C. W. J. Beenakker, *ibid.* **62**, 2020 (1989); C. Zhang and R. R. Gerhardts, Phys. Rev. B **41**, 12850 (1990); R. R. Gerhardts, *ibid.* **45**, 3449 (1991).

[17] D. R. Hofstadter, Phys. Rev. **14**, 2239 (1976); M. Wilkinson, J. Phys. A: Math. Gen. **17**, 3459 (1984); **20**, 4337 (1987); **23**, 2529 (1990); R. Rammal and J. Bellissard, J. Phys. France **51**, 1803 (1990); D. J. Thouless, in *The quantum Hall Effect*, 2nd Ed., edited by R. E. Prange and S. M. Girvin (Springer-Verlag, New York, 1990).

[18] P. D. Ye *et al.*, J. Appl. Phys. **67**, 1441 (1995); P. D. Ye, D. Weiss, and R. R. Gerhardts, J. Appl. Phys. **81**, 5444 (1997). Some experimental indications of the fractal structure in 2DEM systems can be found in R. R. Gerhardts, D. Weiss, and U. Wulf, Phys. Rev. **B43**, 5192 (1991); I. N. Harris *et al.*, Europhys. Lett. **29**, 333 (1995).

[19] R. Alicki, J. R. Klauder, and J. Lewandowski, Phys. Rev. A **48**, 2538 (1993). Alicki *et al.* extend Dubrovin and Novikov's result[14] to a more general case, where the 2DEG lives on a general 2D curved surface with a non-uniform magnetic field everywhere perpendicular to the surface.

[20] L. D. Landau and E. M. Lifshitz, *Quantum Mechanics*, (Pergamon Press, Oxford, 1985).

[21] J. Zak Phys. Rev. **136**, A776 (1964); **134**, A1602 (1964).

[22] A similar multi-band calculation has been done recently for the 2DEM systems by using a matrix continued fraction expansion, see G. Petschel and T. Geisel, Phys. Rev. Lett.

71, 239 (1993). Also see D. Springsguth, R. Ketzmerick, and T. Geisel, Phys. Rev. B **56**, 2036 (1997).

[23] Y. Aharonov and A. Casher, Phys. Rev. A **19**, 2461 (1979). In this paper, the authors show that the zero-energy states always exist for a 2DEG under a *localized* non-uniform magnetic field.

[24] L. E. Gendenshtein, Sov. J. Nucl. Phys. **41**, 166 (1985).

[25] M. J. Snelling *et al.*, Phys. Rev. B **44**, 11345 (1991); R. M. Hannak *et al.*, Solid State Commun. **93**, 3132 (1995).

[26] D. K. Maude *et al.*, Phys. Rev. Lett. **77**, 4604 (1996).

[27] J. Rammer and A. L. Shelankov, Phys. Rev. B **36**, 3135 (1987).

[28] M. C. Chang, M. F. Yang, and T. M. Hong, Phys. Rev. B **56**, 3602 (1997) and the references therein.

FIGURES

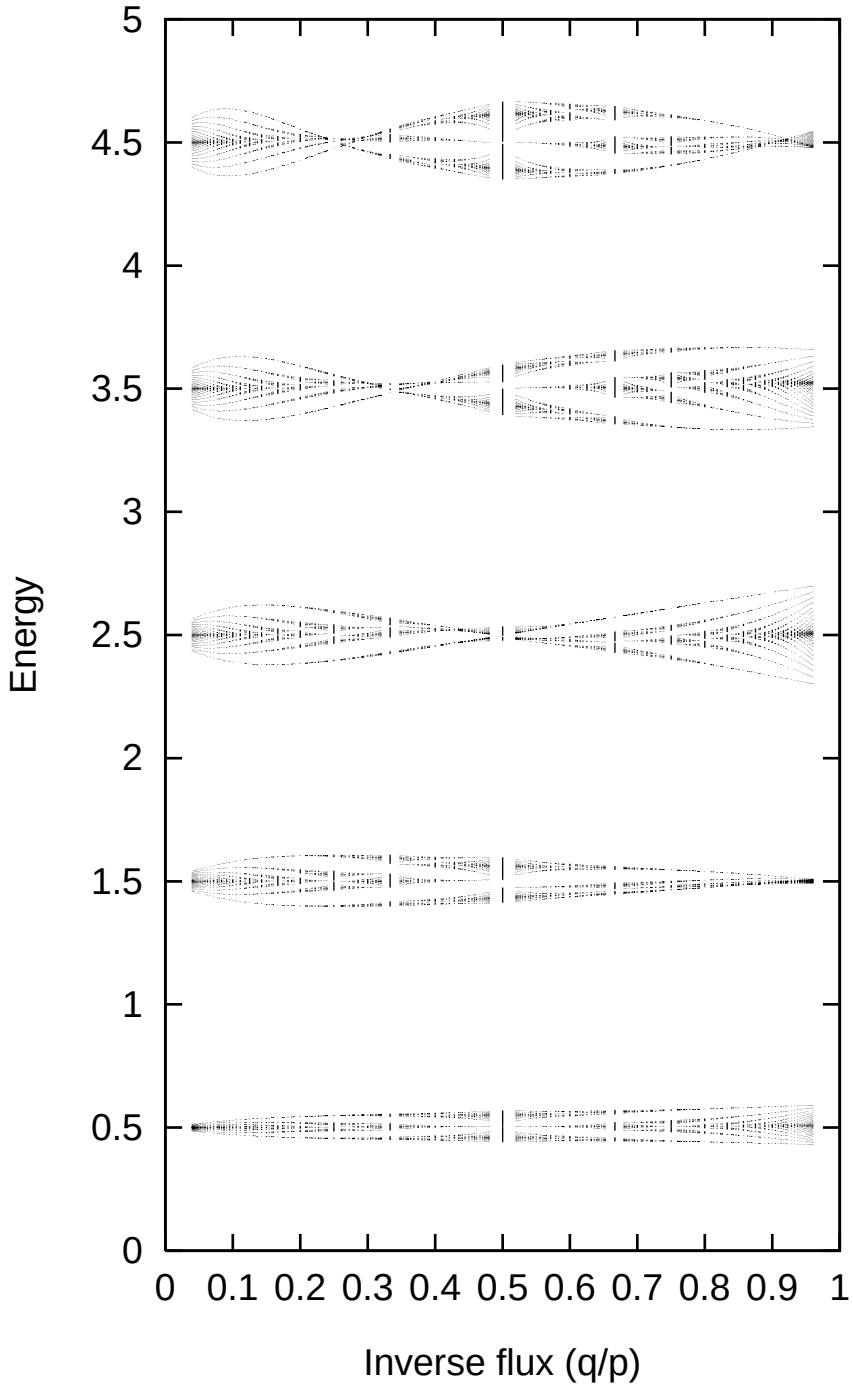
FIG. 1. The lowest five energy bands for spin-down electrons with $g_e = 0$ under a weak square modulation field. The modulation strength is fixed at $b_{10}a^2 = 0.2\phi_0$ while the total flux per plaquette, B_0a^2, varies. The energy is in units of $\hbar\omega_c$ and the inverse flux per plaquette is in units of ϕ_0^{-1}.

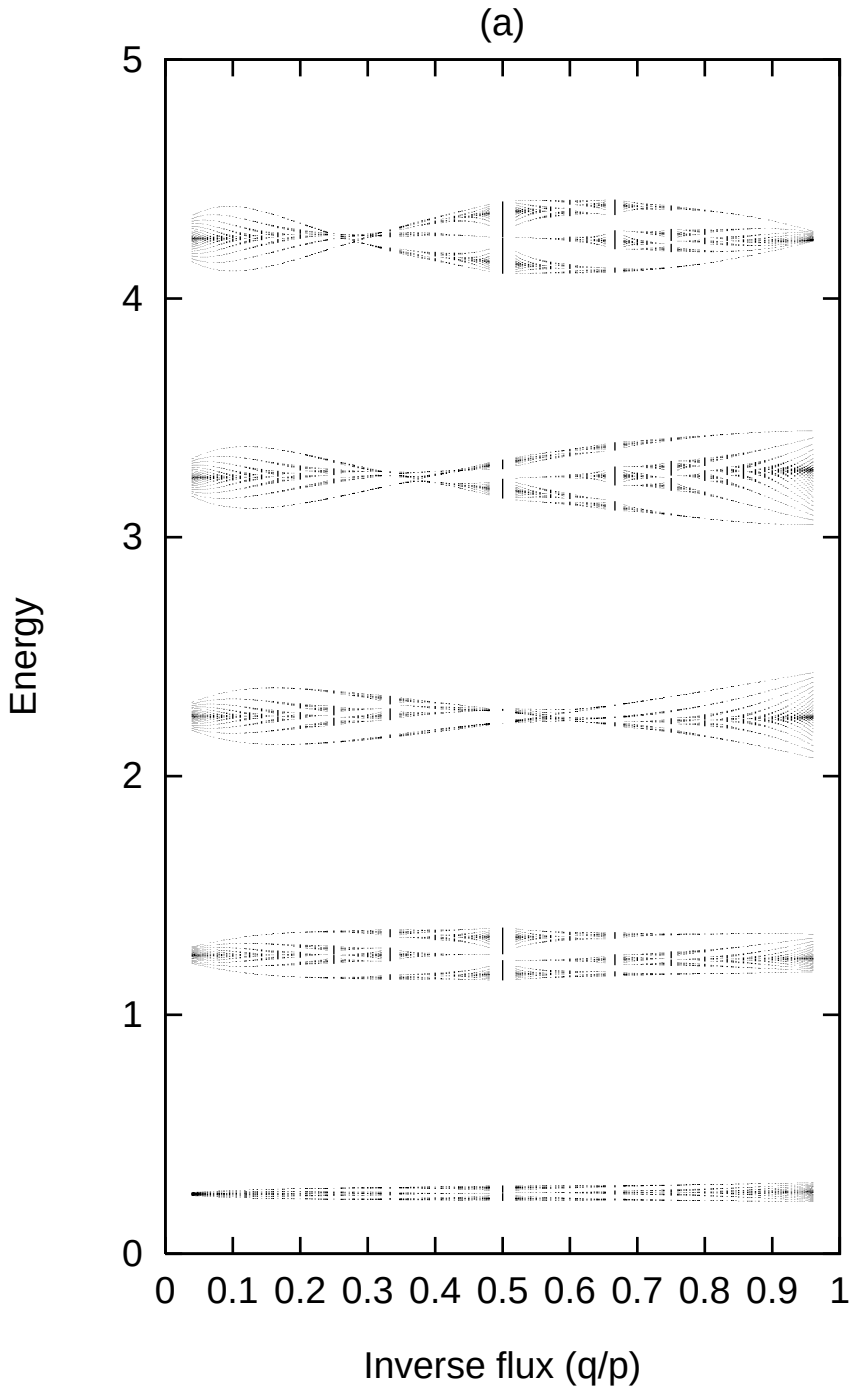
FIG. 2. The lowest five energy bands for a spin-down (a) and a spin-up (b) electrons with $g_e = 1$. The modulation strength and the units being used are the same as those in Fig. 1.

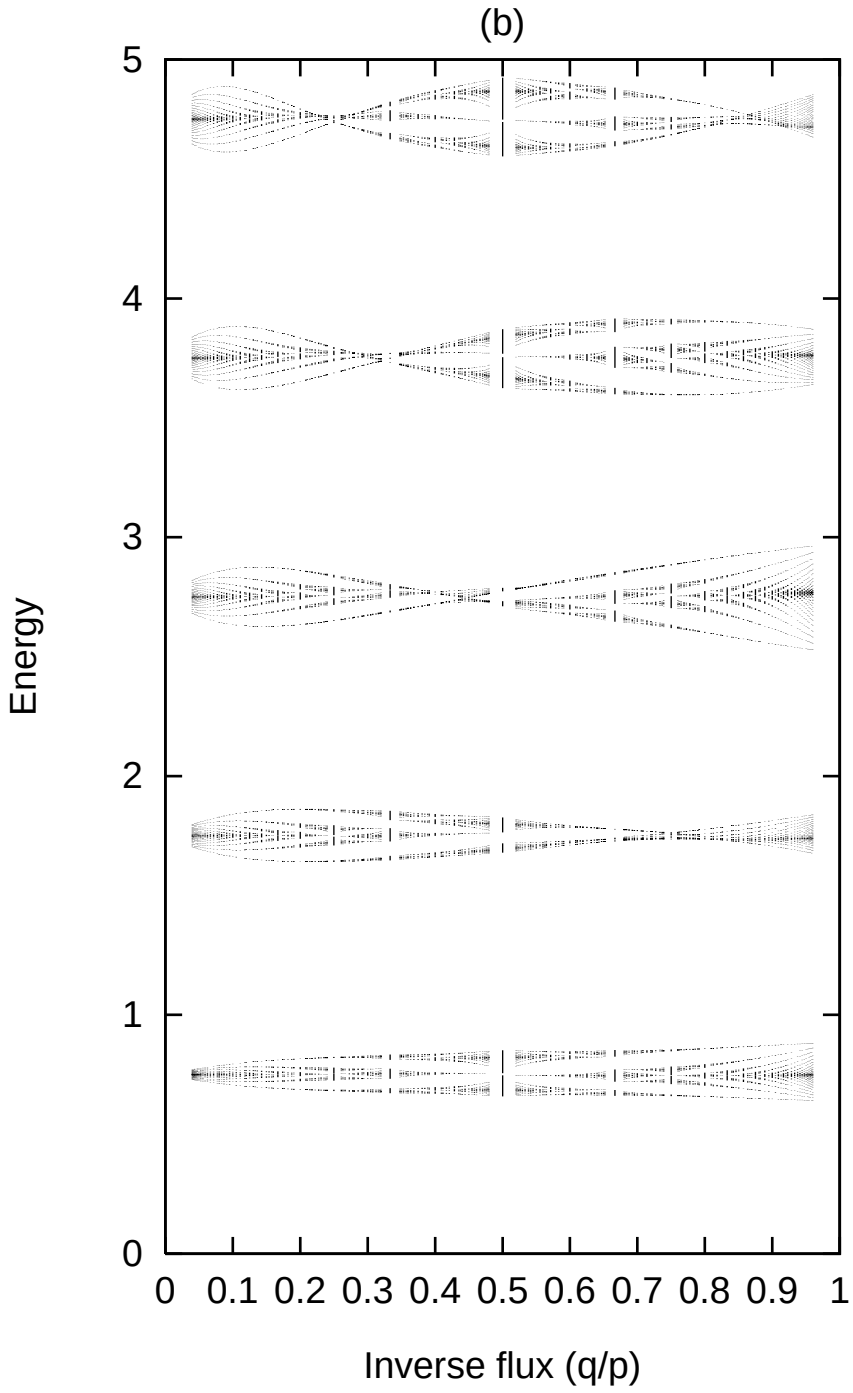
FIG. 3. The lowest five energy bands for a spin-down (a) and a spin-up (b) electrons with $g_e = 2$. The modulation strength and the units being used are the same as those in Fig. 1. It can be seen that the lowest energy level for a spin-down electron is flat. Also, the spectrum is degenerate with respect to spin flip, except for the zero-energy flat band in (a).

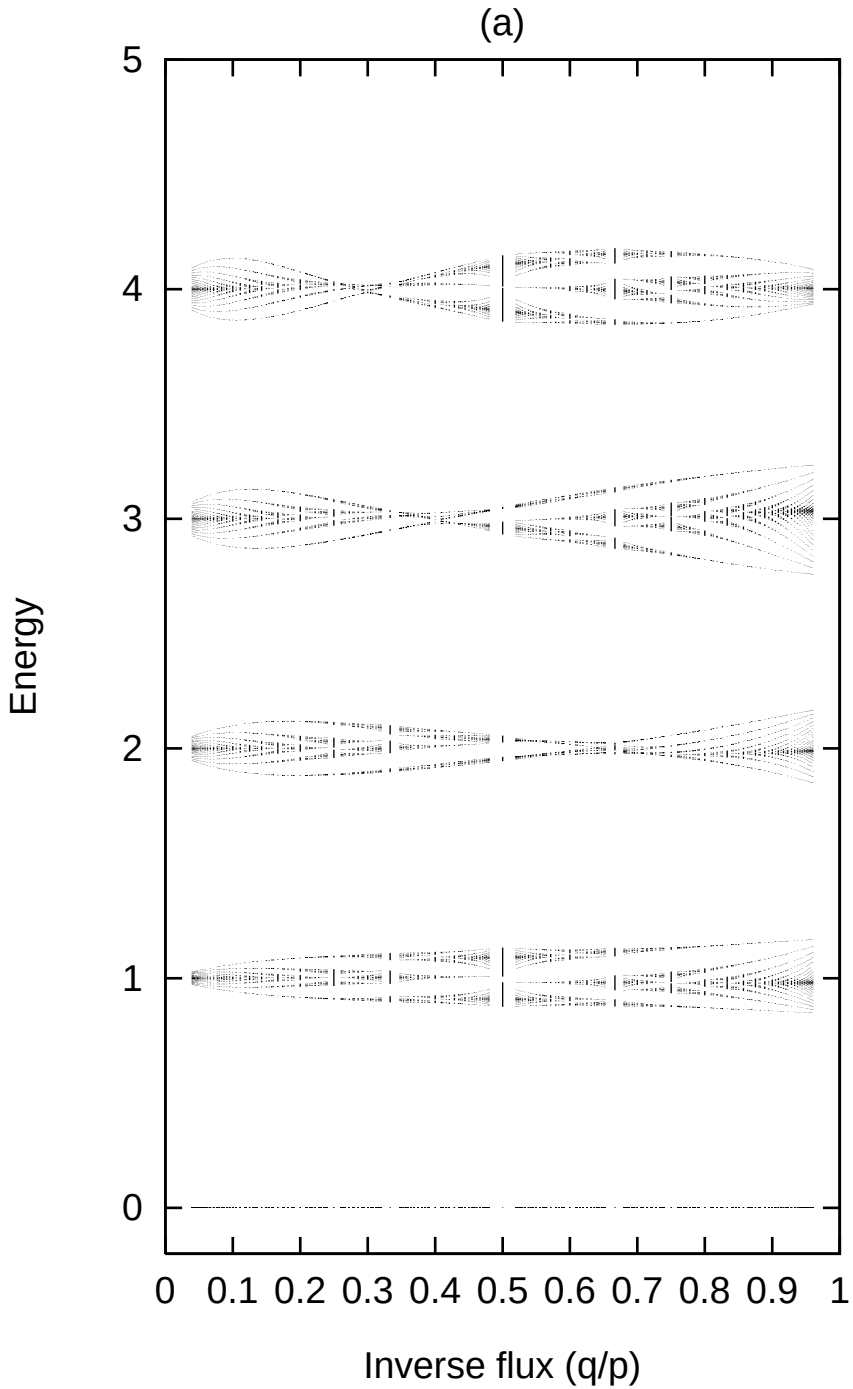
FIG. 4. The lowest five energy bands for a spin-down electron with $g_e = 1$ (a) and 2 (b). The modulation strength is $b_{10}a^2 = 0.8\phi_0$.

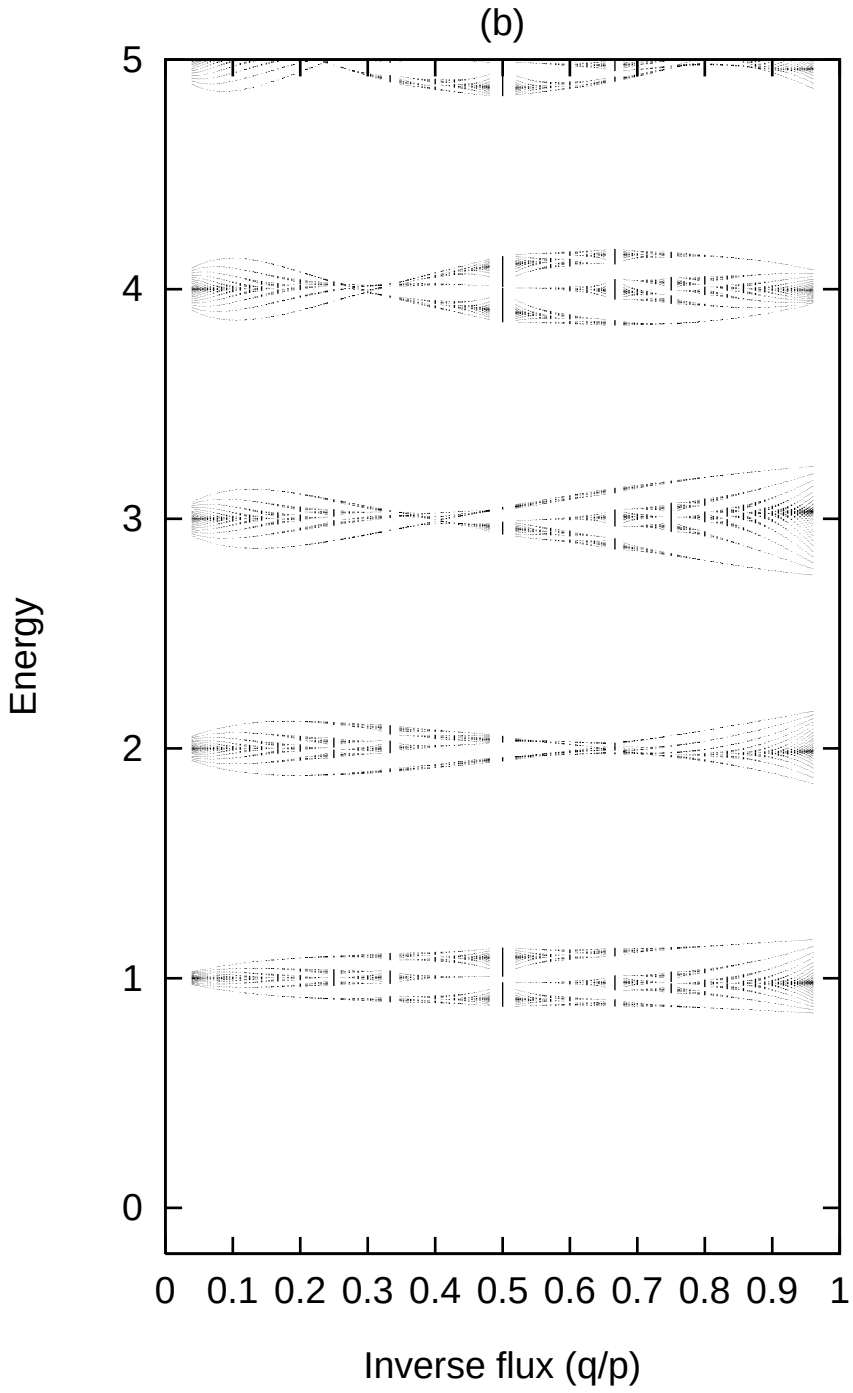
FIG. 5. The dependence of the band widths on the g factor when the total flux per plaquette $B_0a^2 = 1\phi_0$ and $b_{10}a^2 = 0.2\phi_0$. The sign of the g factor refers to the direction of spins (+ for up, − for down). The energy bands at $g_e = -2$ are indicated by vertical bold lines.

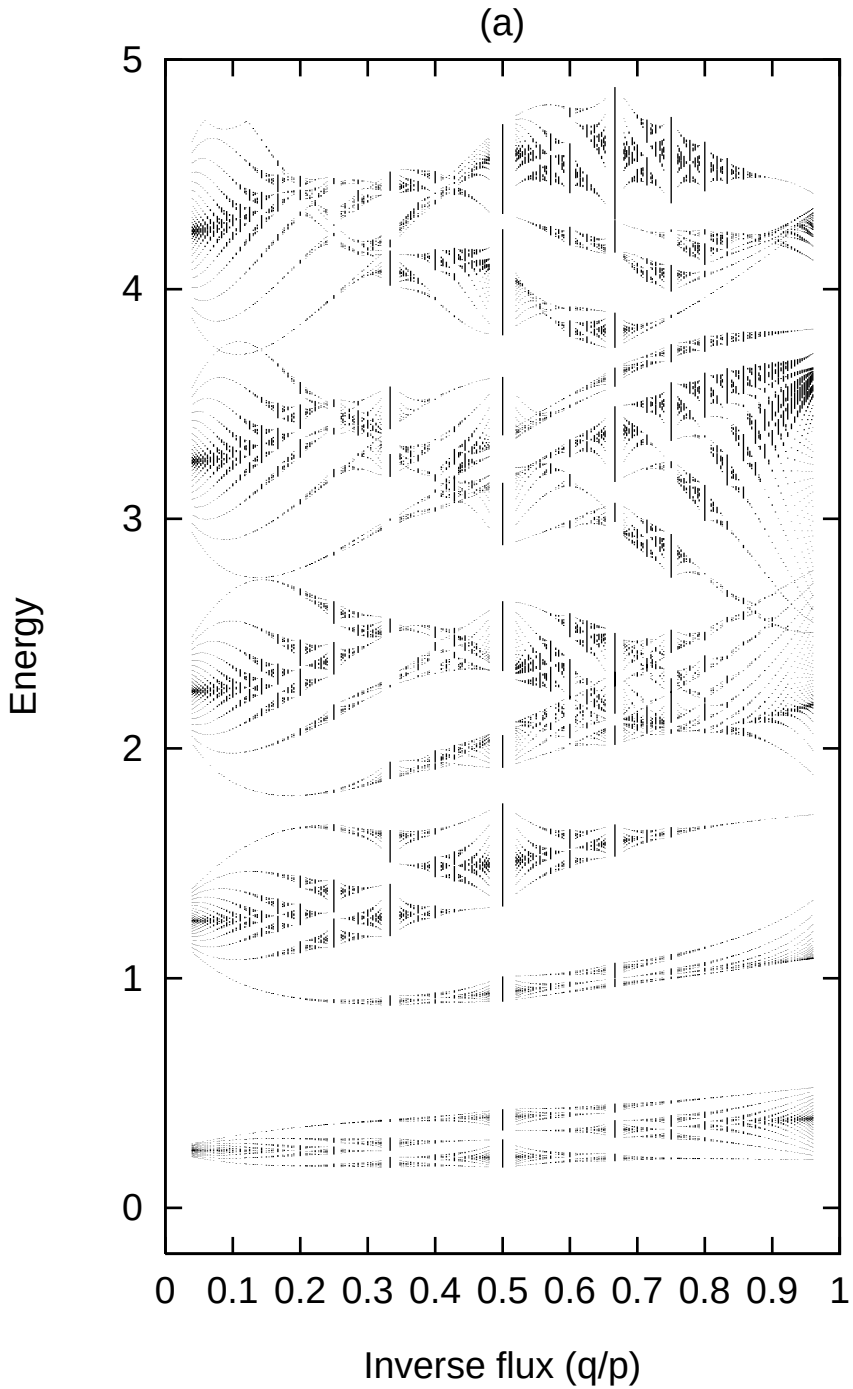

Energy
Inverse flux (q/p)
0
0.5
1
1.5
2
2.5
3
3.5
4
4.5
5
0
0.1
0.2
0.3
0.4
0.5
0.6
0.7
0.8
0.9
1

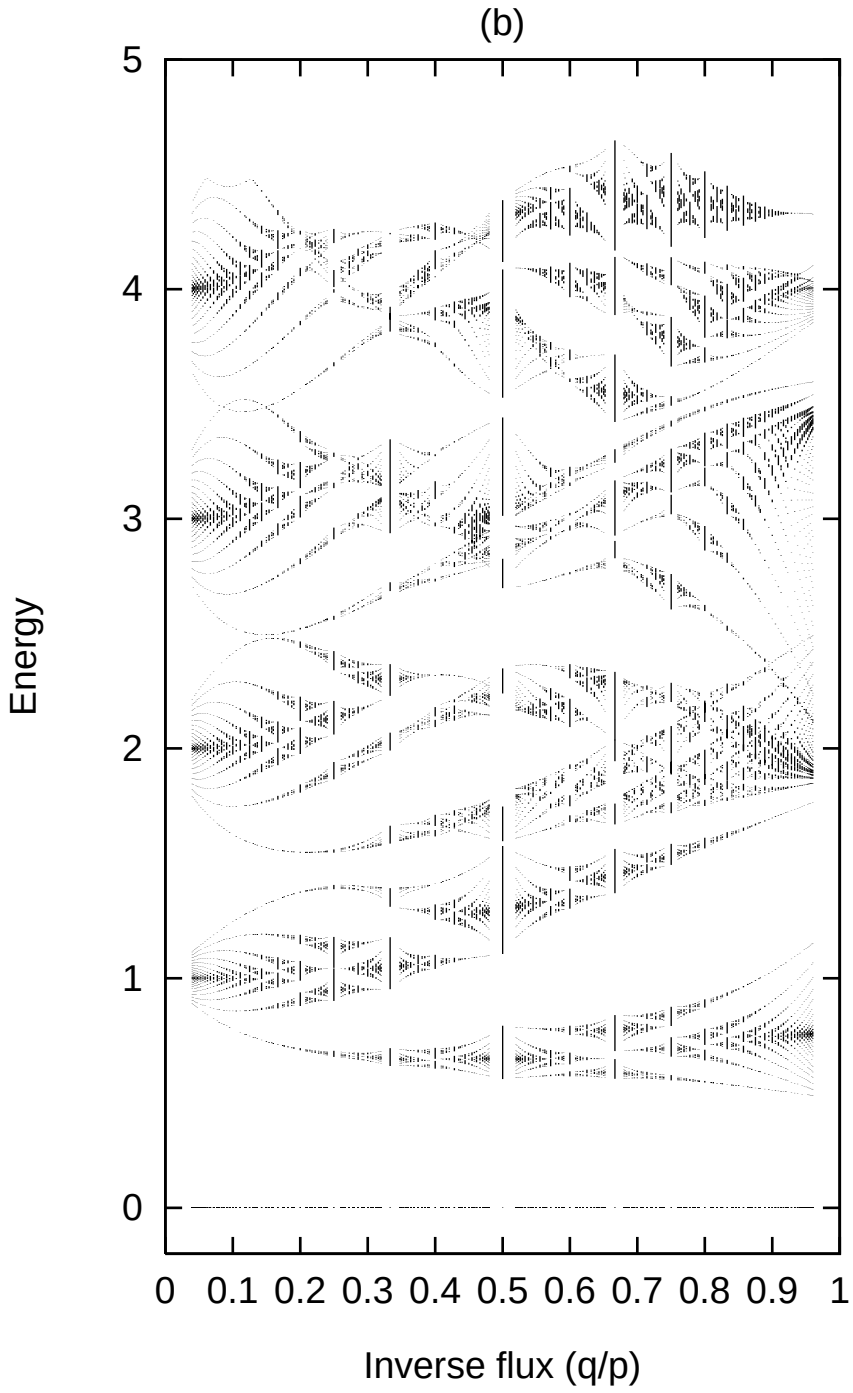

(a)
Energy
Inverse flux (q/p)
0
1
2
3
4
5
0
0.1
0.2
0.3
0.4
0.5
0.6
0.7
0.8
0.9
1

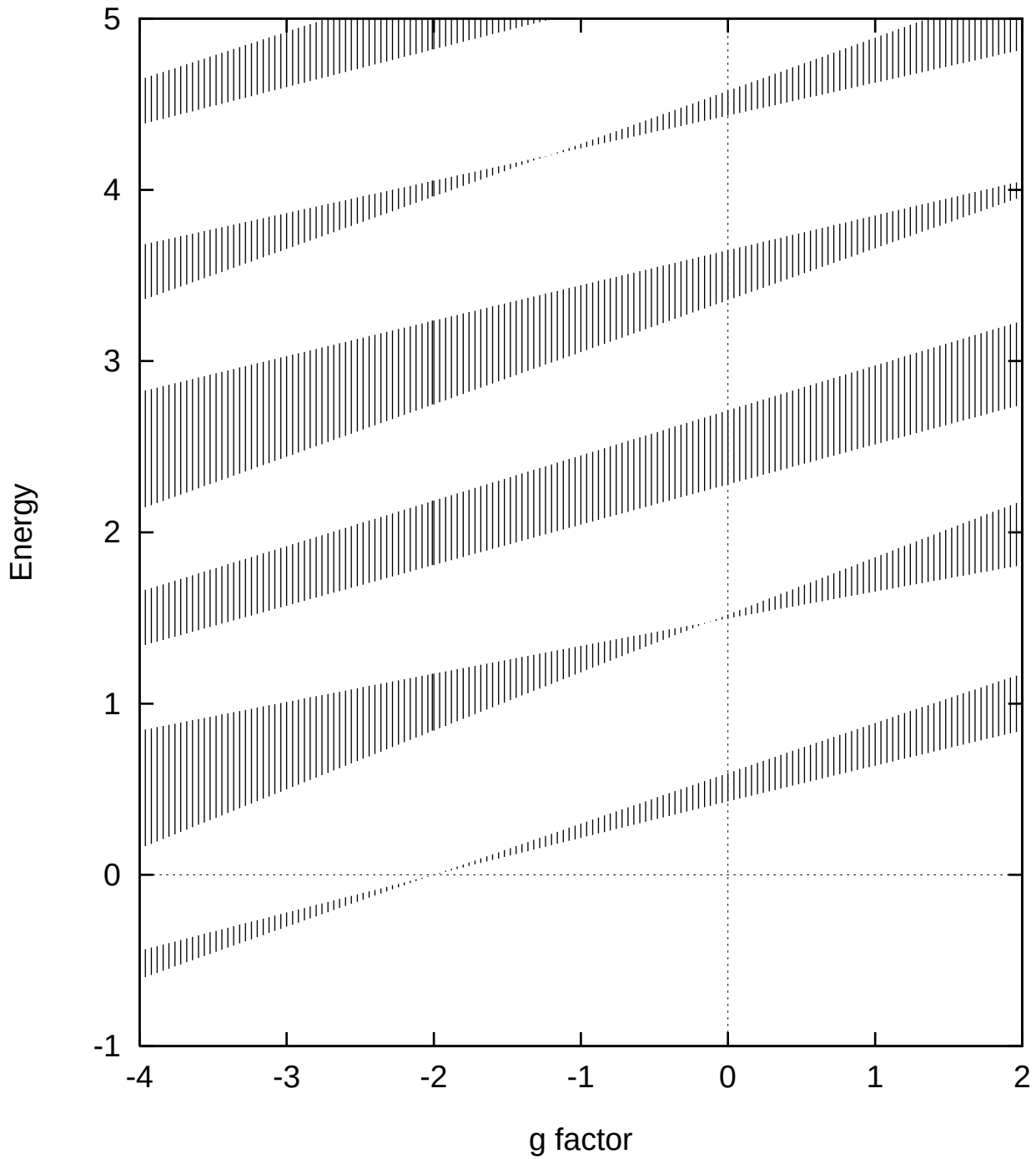

(b)
Energy
Inverse flux (q/p)
0
1
2
3
4
5
0
0.1
0.2
0.3
0.4
0.5
0.6
0.7
0.8
0.9
1


(a)
5
4
3
2
1
0
Energy
0
0.1
0.2
0.3
0.4
0.5
0.6
0.7
0.8
0.9
1
Inverse flux (q/p)


(b)
Energy
Inverse flux (q/p)
0
1
2
3
4
5
0
0.1
0.2
0.3
0.4
0.5
0.6
0.7
0.8
0.9
1


(a)
Energy
Inverse flux (q/p)
0
1
2
3
4
5
0
0.1
0.2
0.3
0.4
0.5
0.6
0.7
0.8
0.9
1


(b)
Energy
Inverse flux (q/p)
0
1
2
3
4
5
0
0.1
0.2
0.3
0.4
0.5
0.6
0.7
0.8
0.9
1


Energy
g factor
5
4
3
2
1
0
-1
-4
-3
-2
-1
0
1
2